Electronic Supplementary Material (ESI) for Organic & Biomolecular Chemistry.

Electronic Supplementary Information

Benzothiazole-based dual reaction site fluorescent probe for the selective detection of hydrazine in water and live cells

Anwesha Maiti,[a] Saikat Kumar Manna,[b] Satyajit Halder,[c] Moumi Mandal,[a] Anirban Karak,[a] Dipanjan Banik,[a] Kuladip Jana,[c] and Ajit Kumar Mahapatra [a*]

[a] Department of Chemistry, Indian Institute of Engineering Science and Technology, Shibpur, Howrah-711103, West Bengal, India, E-mail: akmahapatra@chem.iiests.ac.in

[b] Department of Chemistry, Haldia Government College, Debhog, Haldia, Purba Medinipur-721657, West Bengal, India.

[c] Division of Molecular Medicine, Bose Institute, P 1/12, CIT Scheme VIIM, Kolkata-700054, India.

Table of Contents

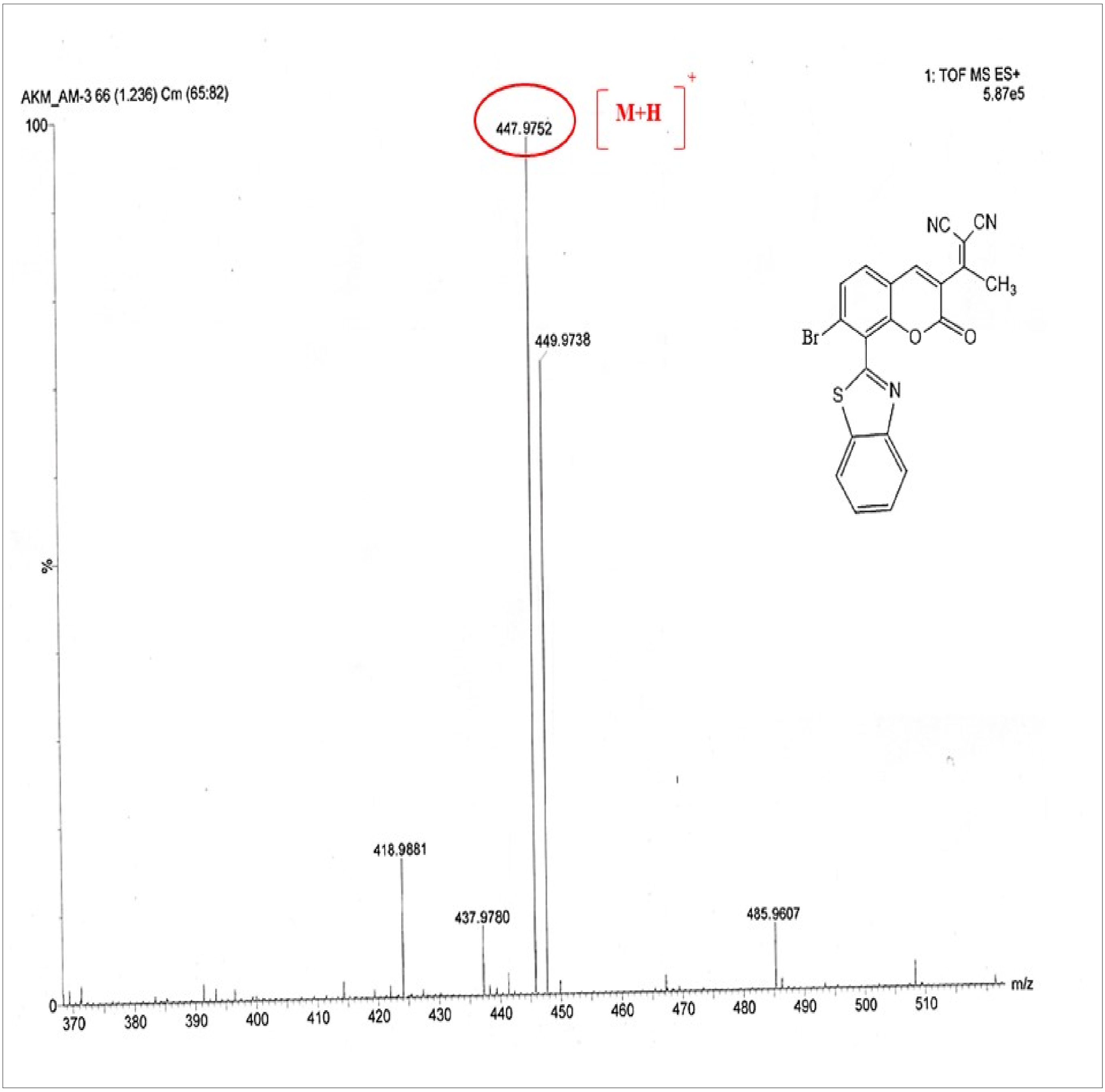

Figure S1: HRMS spectrum of probe BTC.

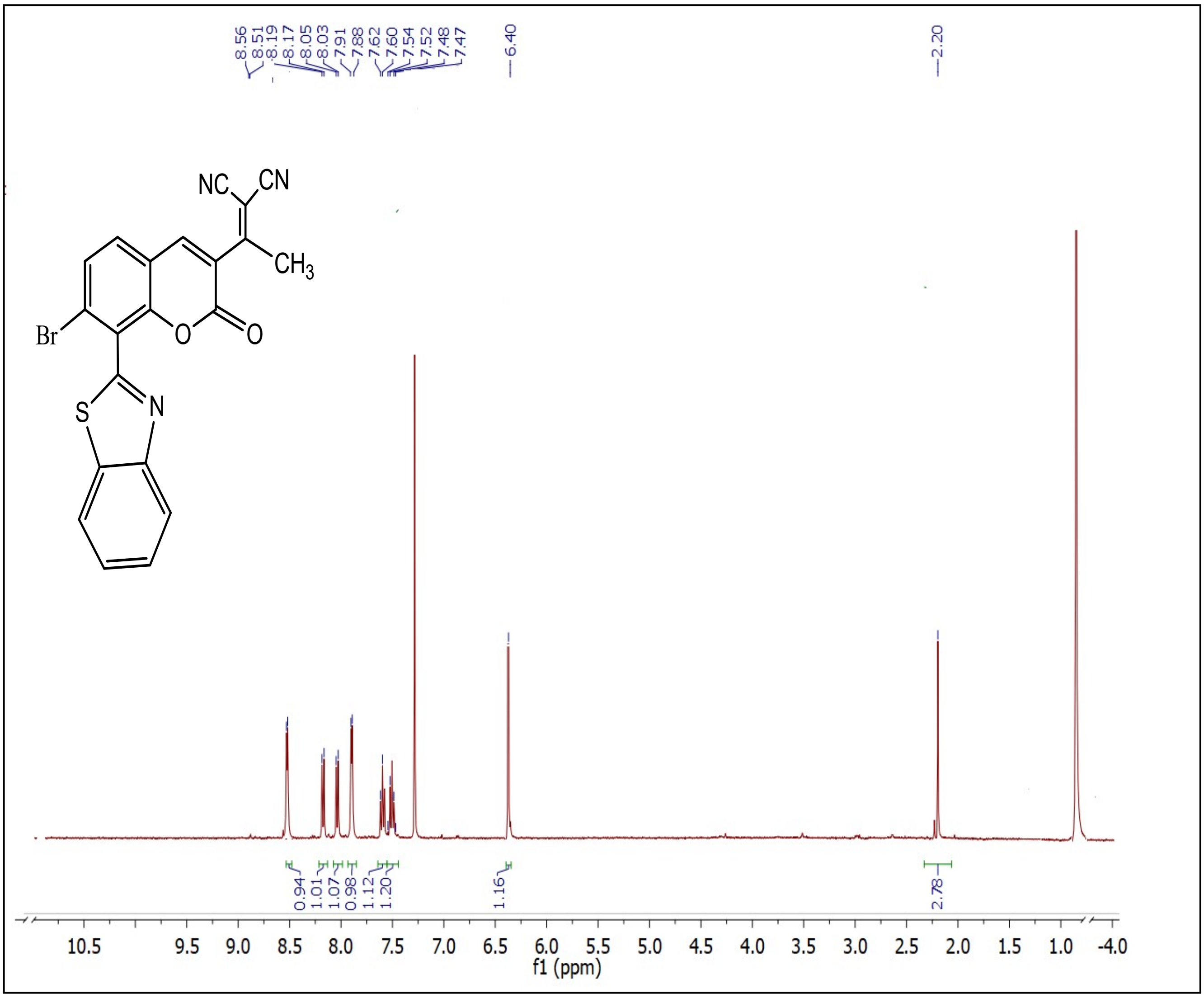

Figure S2: ^{1}H NMR spectrum of probe BTC in $CDCl_3$.

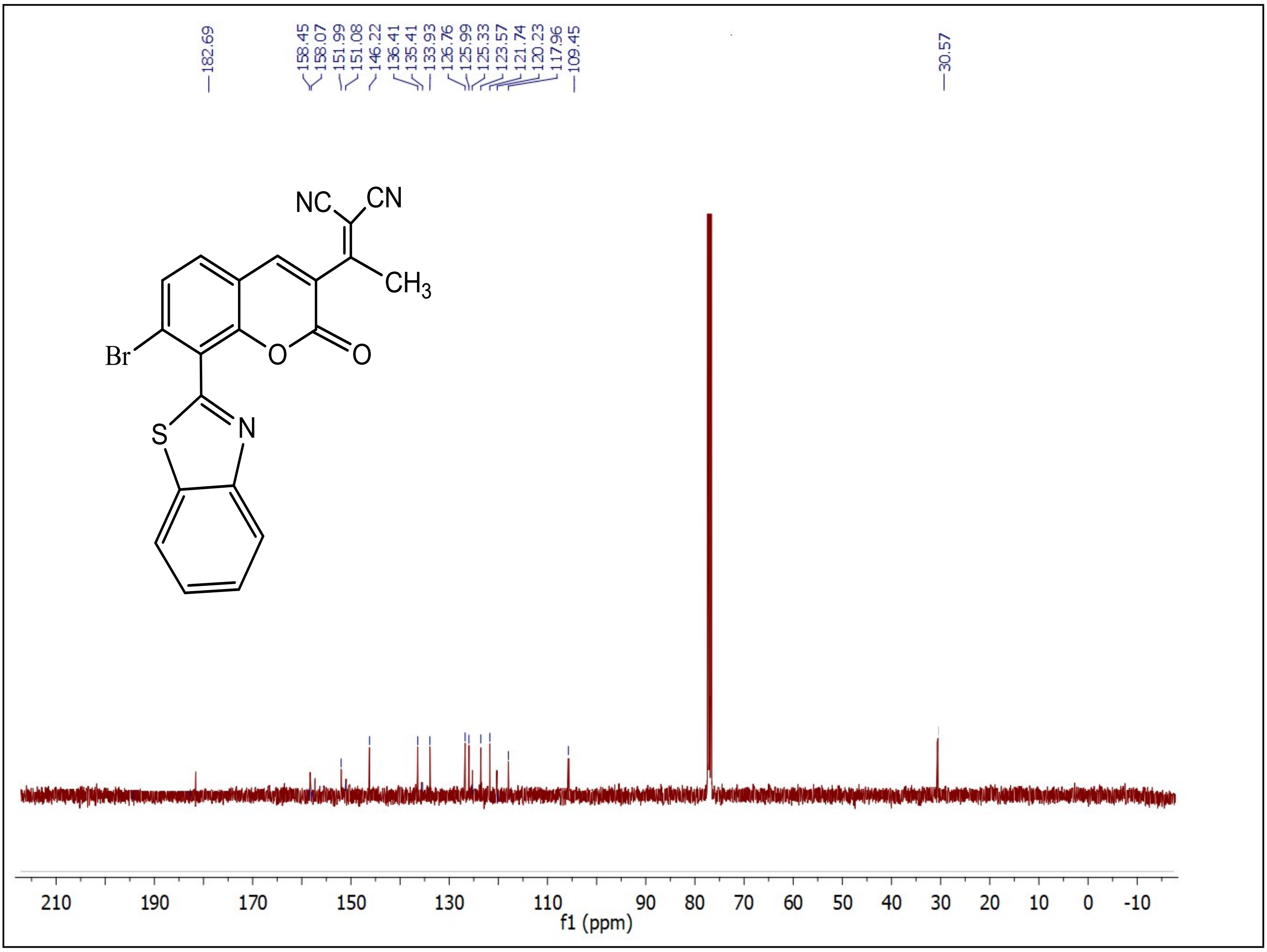

Figure S3: ^{13}C NMR spectrum of probe BTC in $CDCl_3$.

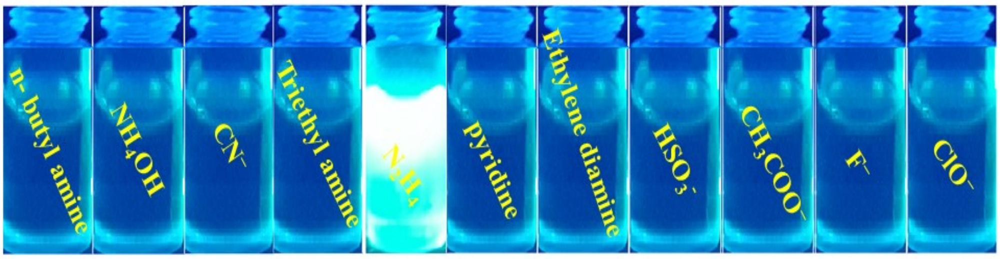

Figure S4: Fluorescence color changes of receptor **BTC** in aq. DMSO (DMSO: H_2O = 7:3 v/v, 10mM HEPES buffer, pH = 7.4) upon addition of various analytes (1) n-butyl amine; (2) NH_2OH; (3) CN^- (4) triethyl amine (5) N_2H_4, (6) pyridine (7) ethylenediamine, (8) HSO_3^-, (9) CH_3COO^- (10) F^- (11) ClO^-.

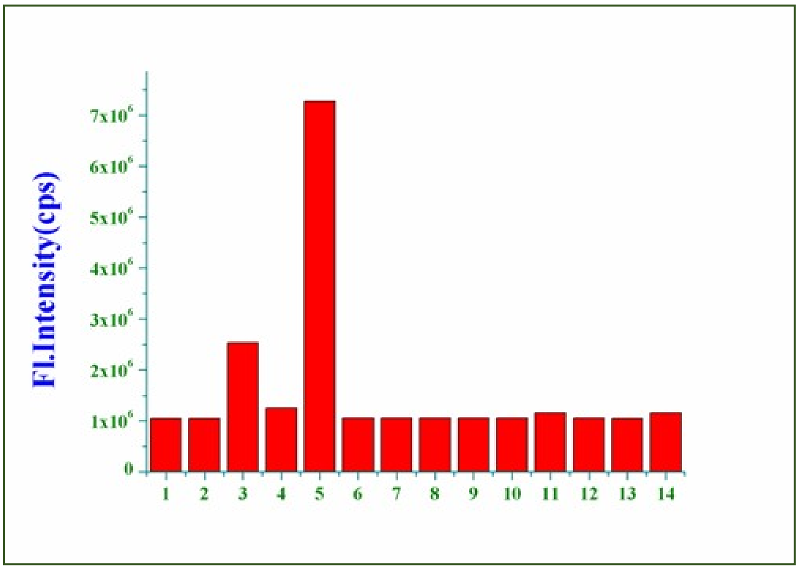

Figure S5: Competitive fluorescence emission spectra of compound **BTC** in the presence of different anions in aq. DMSO (DMSO /H_2O) = 7:3 solution.

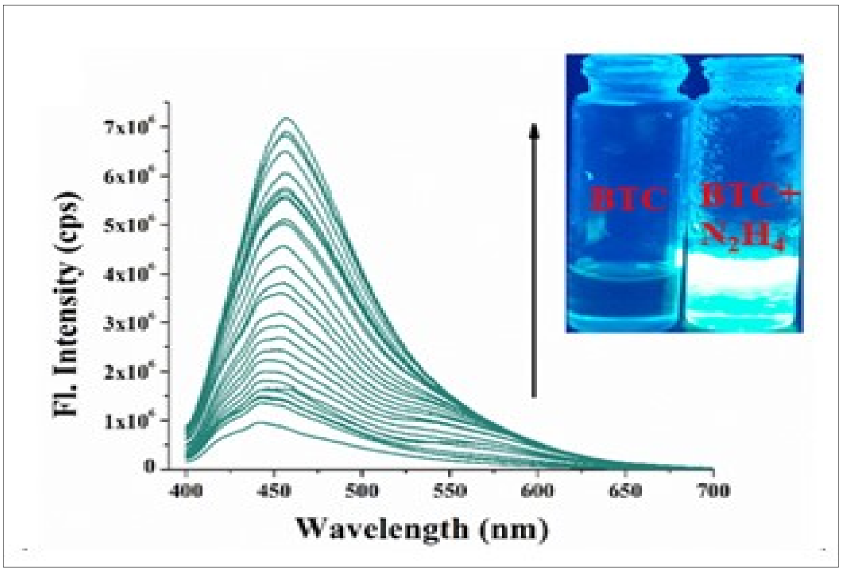

Figure S6: Fluorescence emission spectrum obtained of **BTC** (c = 4×10^{-5} M) with N_2H_4 (c = 4×10^{-4} M) in aqueous DMSO (DMSO /H_2O = 7:3 v/v, 10 mM HEPES buffer)

pH effect:

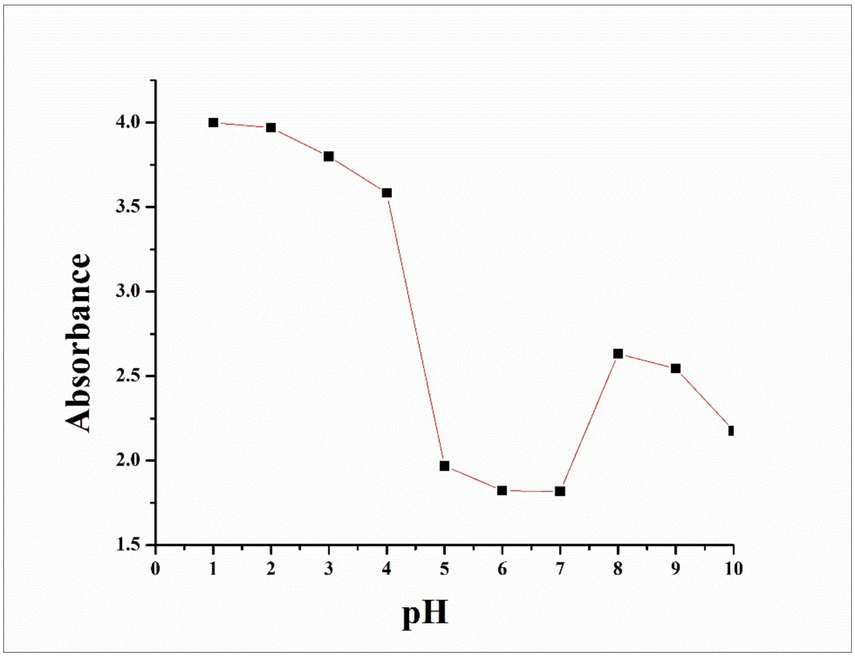

Figure S7: pH-dependent changes in the absorbance of probe **BTC** (1×10^{-5} M) in presence of hydrazine (1×10^{-4} M) in DMSO-H_2O (DMSO /H_2O = 7:3 v/v, 10 mM HEPES buffer, pH = 7.4)

Calculation of Detection limit:

The detection limit (DL) of **BTC** for N_2H_4 were determined from the following equation: DL = K*Sb1/S; Where K= 2 or 3 (we take 2 in this case); Sb1 is the standard deviation of the blank solution; S is the slope of the calibration curve.

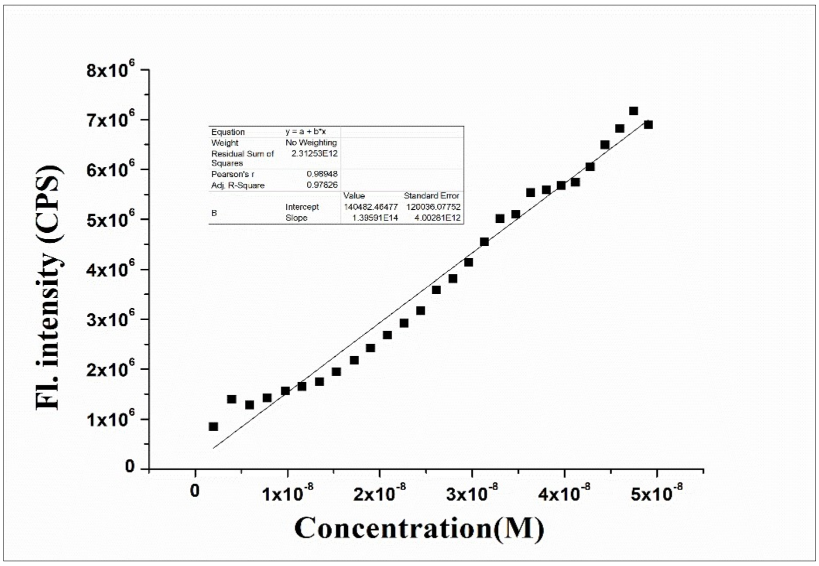

Figure S8 : From the graph we get slope (S) = 1.39591×10^{14}, Standard deviation (Sb1=120036.07752). Thus, using the formula, we get the detection limit = 1.7 nM

Kinetic study of probe BTC:

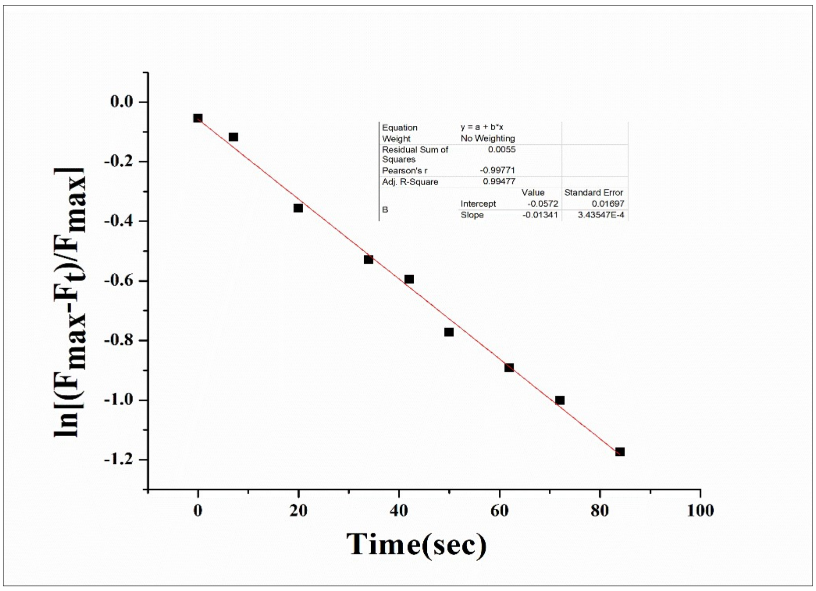

Figure S9 : Pseudo first order kinetic diagram of probe **BTC** (1×10^{-5} M) with $\mathbf{N_2H_4}$ (1×10^{-4} M) in DMSO-H_2O

Computational details:

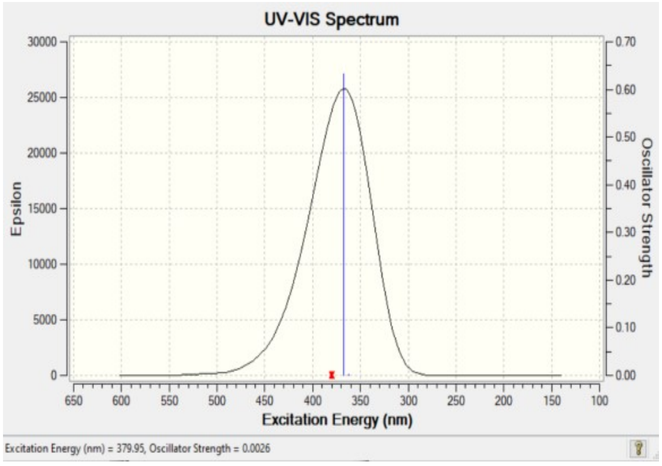

Figure S10 : Absorption spectra of the probe **BTC**

Table S1: The vertical main orbital transition of probe calculated by TD-DFT method

Energy(eV)	**Wavelength (nm)**	**Osc. strength(f)**	**Transition**
3.2632	379.95	0.0026	**HOMO→LUMO**
3.3762	367.23	0.6333	**HOMO-2→LUMO**
3.4207	362.45	0.0015	**HOMO-1→LUMO**

Calculation of fluorescence quantum yield of BTC-N_2H_4 adduct:

Here, the fluorescence quantum yield Φ was calculated by using the following equation:

$\Phi_x = \Phi_s (F_x / F_s) (A_s / A_x) (\eta_x^2 / \eta_s^2)$

Where,

X and S indicate the unknown and standard solution respectively, Φ = quantum yield

F = Area under the emission curve, A= Absorbance at the excitation wavelength,

η = Refractive index of solvent. Here Φ measurements were performed using fluorescein in ethanol as standard [Φ = 0.79]

The fluorescence quantum yield of **BTC-N_2H_4** product was calculated by taking fluorescein (Φ = 0.79 in ethanol) as standard.

η_s = 1.3614 (for ethanol); η_x = 1.479 (for DMSO)

The quantum yield of **BTC-N_2H_4** adduct was calculated using the above equation and the value is 0.67.

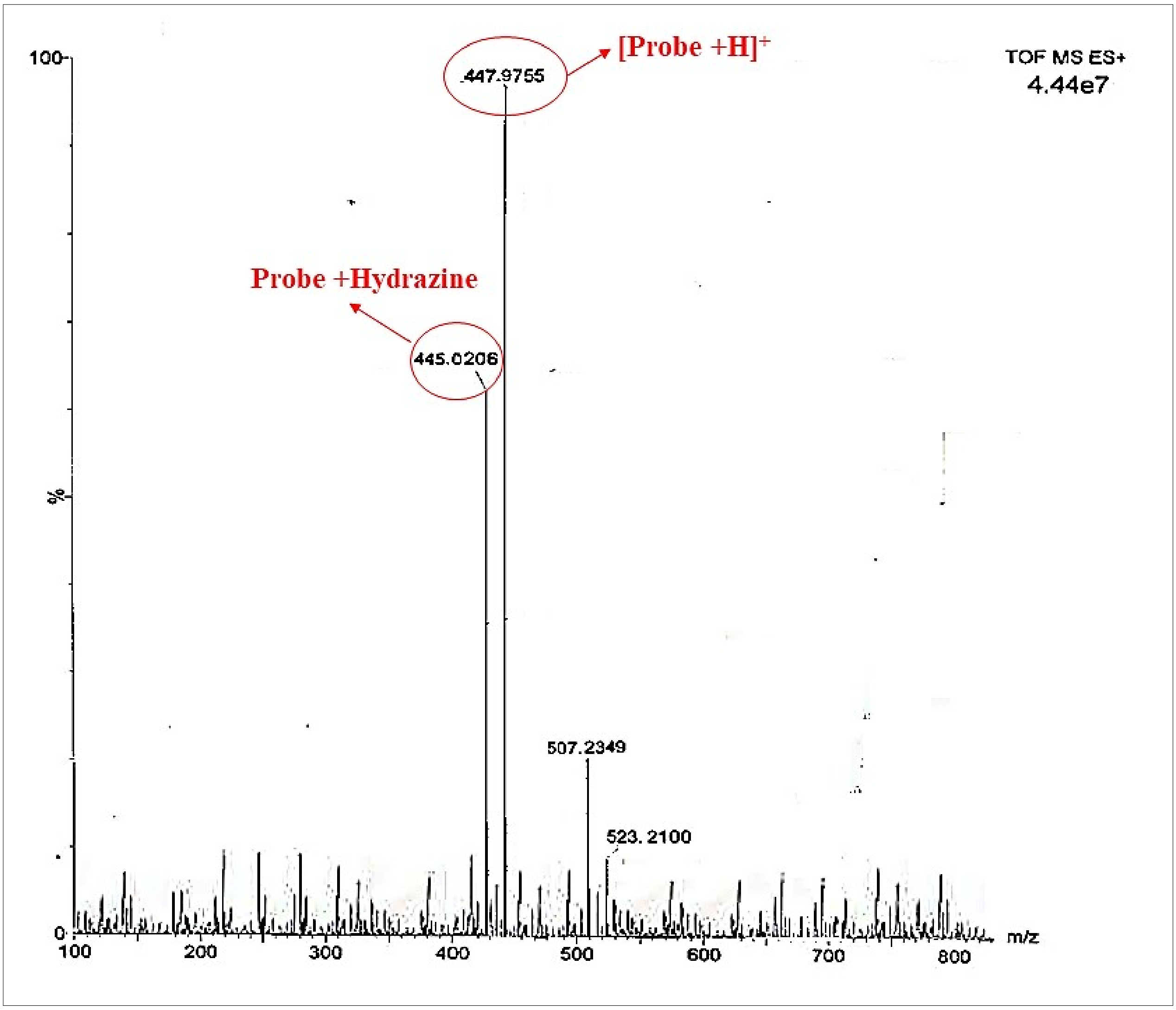

Figure S11: HRMS of BTC-N_2H_4 adduct in assay.

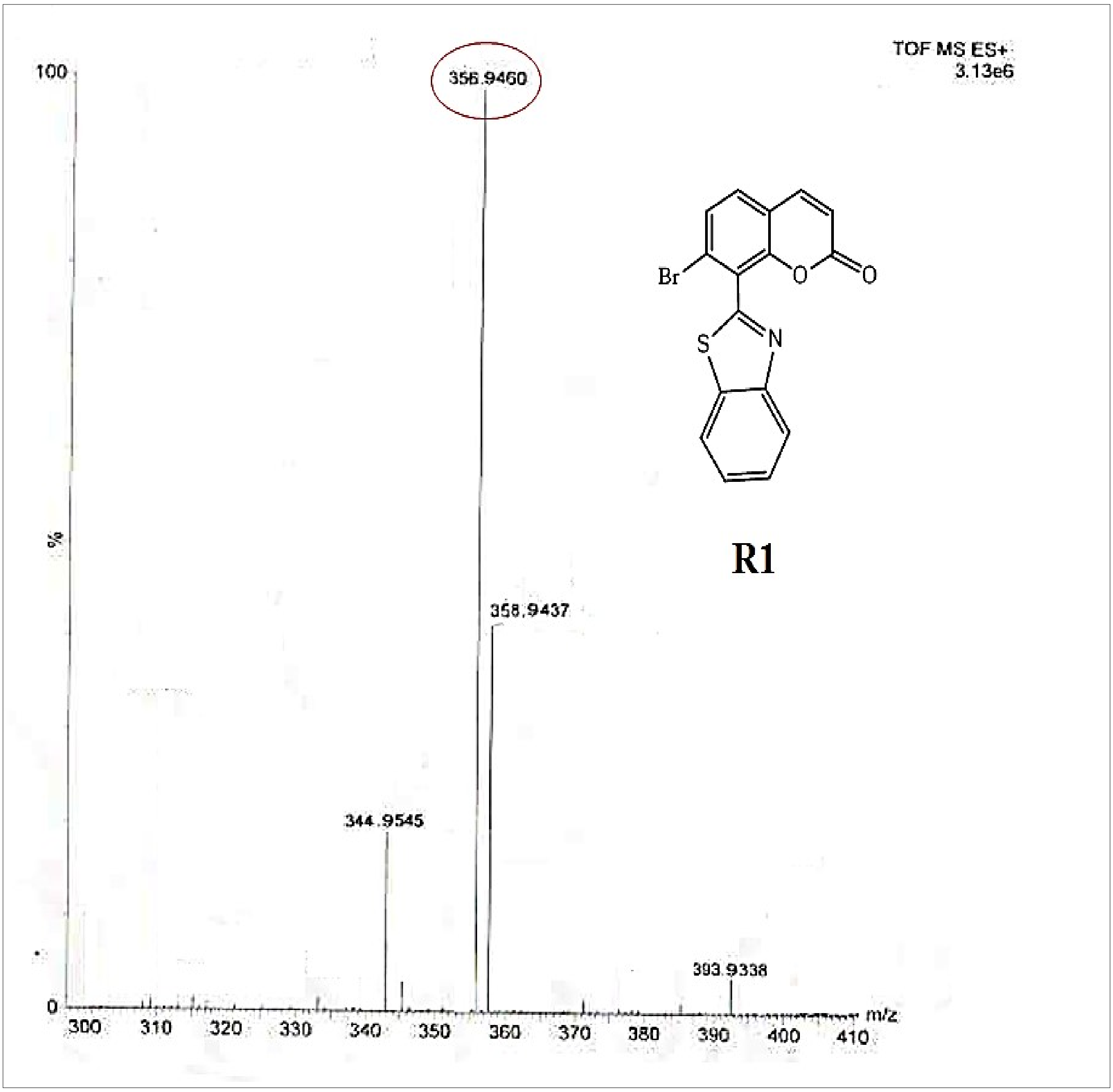

Figure S12: HRMS of reference compound R1.

Table S2: Comparison data of previously reported N_2H_4 sensors with current data

Sl. No.	Probe structure	Excitation	Emissioon in presence of hydrazine	Detec tion limit	Response time	Application	Reference
1.	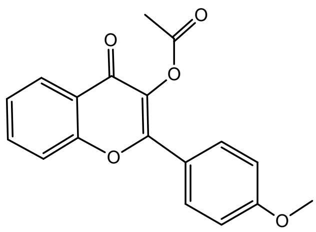	370 nm	415 nm (N* form) and 540 nm (T* form)	10 µM	60 min	Live stem cell and *in vivo* zebrafish imaging	[1]
2.	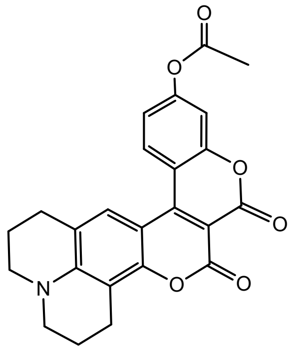	480 nm	542 nm	5.4 ppb	10 min	Live HeLa cell and *in vivo* zebrafish imaging	[2]
3.	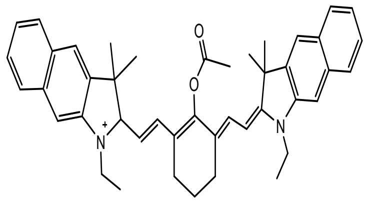	540 nm and 730 nm	662 nm to 825 nm	2.56 ppb	7 min	Live cell, kidney and in vivo mouse body imaging	[3]
4.	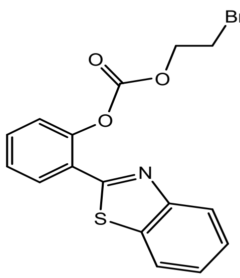	300 nm	368 nm to 458 nm	0.78 ppb	1 h	Live cell imaging	[4]
5.	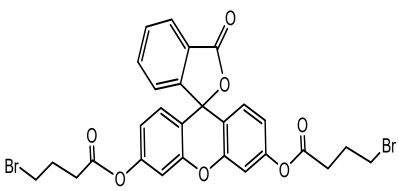	460 nm	516 nm	3.2 ppb	30s	No application	[5]

6.	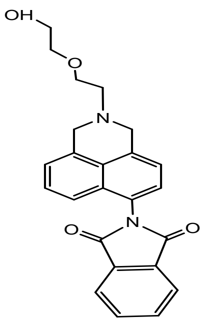	405 nm	467 nm to 528 nm	4.2 nM	15 min	Live HeLa cell imaging	[6]
7.	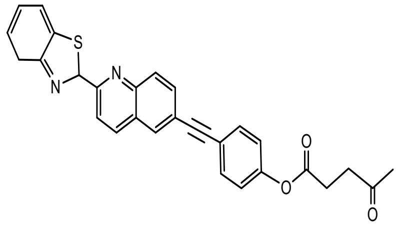	365 nm	414 nm to 460 nm	0.22 ppb	5 min	No application	[7]
8.	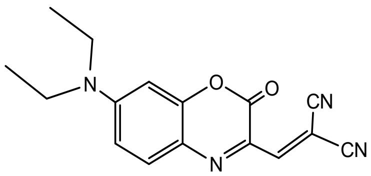	510 nm	639 nm to 564 nm	0.43 µM	20 min	Live HeLa cell imaging	[8]
9.	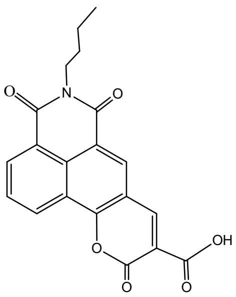	320 nm and 470 nm	435 nm to 560 nm	36 nM	5 min	Live cell imaging and vapor phase detection by test strips.	[9]
10.	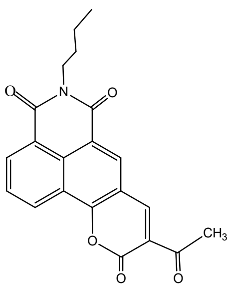	400 nm	471 nm to 560 nm	0.2032 µM	10 min	Live cell imaging and vapor phase detection by test strips.	[10]
11.	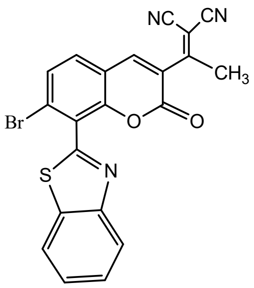	390 nm	446 nm	1.7 nM	1 min	Live cell imaging and vapor phase detection by test strips.	Our Work

References:

[1] B. Liu, Q. Liu, M. Shah, J. Wang, G. Zhang and Y. Pang, *Sens. Actuators, B*, 2014, **202**,194–200.

[2] Q. Fang, L. Yang, H. Xiong, S. Han, Y. Zhang, J. Wang, W. Chen and X. Song, *Chinese Chem. Lett*., 2019, 2–5.

[3] Y. Song, G. Chen, X. Han, J. You and F. Yu, *Sens. Actuators, B*, 2019, **286**, 69–76.

[4] S. Goswami, S. Das, K. Aich, B. Pakhira, S. Panja, S.K. Mukherjee and S. Sarkar, *Org. Lett.*, 2013, **15**, 5412–5415.

[5] S. Goswami, K. Aich, S. Das, S. Basu Roy, B. Pakhira and S. Sarkar, *RSC Adv*., 2014, **4**, 14210–14214.

[6] M.V. Ramakrishnam Raju, E. Chandra Prakash, H.C. Chang and H.C. Lin, *Dyes Pigm.*, 2014, **103**, 9–20.

[7] S. Yu, S. Wang, H. Yu, Y. Feng, S. Zhang, M. Zhu, H. Yin and X. Meng, *Sens. Actuators, B*, 2015, **220**, 1338–1345.

[8] J. Fan, W. Sun, M. Hu, J. Cao, G. Cheng, H. Dong, K. Song, Y. Liu, S. Sun and X. Peng, *Chem. Commun*., 2012, **48**, 8117–8119.

[9] W. Zhang, F. Huo, T. Liu and C.Yin, *J. Mater. Chem. B*, 2018, **6**, 8085.

[10] X. Shi, C. Yin, Y. Zhang, Y. Wen and F. Huo, *Sens. Actuators, B*, 2019, **285**, 368– 374.